Energy and density analysis of the H_2 molecule from the united atom to dissociation: The $^3\Sigma_g^+$ and $^3\Sigma_u^+$ states

Giorgina Corongiu[1,a)] and Enrico Clementi[2]
[1]*Dipartimento di Scienze Chimiche e Ambientali, Università dell'Insubria, Via Valleggio 11, I-22100 Como, Italy*
[2]*Via Carloni, 38 22100 Como, Italy*

(Received 10 August 2009; accepted 18 October 2009; published online 12 November 2009)

The first 14 $^3\Sigma_g^+$ and the first 15 $^3\Sigma_u^+$ states of the H_2 molecule are computed with full configuration interaction both from Hartree–Fock molecular orbitals and Heitler–London atomic orbitals within the Born–Oppenheimer approximation, following recent studies for the $^1\Sigma_g^+$ and $^1\Sigma_u^+$ manifolds [Corongiu and Clementi, J. Chem. Phys. **131**, 034301 (2009) and J. Phys. Chem. (in press)]. The basis sets utilized are extended and optimized Slater-type functions and spherical Gaussian functions. The states considered correspond to the configurations $(1s^1nl^1)$ with n from 1 to 5; the internuclear separations sample the distances from 0.01 to 10 000 bohrs. For the first three $^3\Sigma_g^+$ and $^3\Sigma_u^+$ states and for the fourth and fifth $^3\Sigma_g^+$ states, our computed energies at the equilibrium internuclear separation, when compared to the accurate values by Staszewska and Wolniewicz and by Kołos and Rychlewski, show deviations of about 0.006 kcal/mol, a test on the quality of our computations. Motivation for this work comes not only from obtaining potential energy curves for the high excited states of H_2 but also from characterizing the electronic density evolution from the united atom to dissociation to provide a detailed analysis of the energy contributions from selected basis subsets and to quantitatively decompose the state energies into covalent and ionic components. Furthermore, we discuss the origin of the seemingly irregular patterns in potential energy curves in the two manifolds, between 4 and 6–9 bohrs—there are two systems of states: the first, from the united atom to about 4 bohrs, is represented by functions with principal quantum number higher than the one needed at dissociation; this system interacts at around 4 bohrs with the second system, which is represented by functions with principal quantum number corresponding to one of the dissociation products. © *2009 American Institute of Physics*. [doi:10.1063/1.3259551]

I. INTRODUCTION

This work reports computations and an analysis of the potential energy curves (PECs) for the lowest 14 $^3\Sigma_g^+$ states and for the lowest 15 $^3\Sigma_u^+$ states of the H_2 molecule, following a computational approach recently utilized for a study of the $^1\Sigma_g^+$ states[1] and the $^1\Sigma_u^+$ states.[2] Full configuration interaction (CI) computations within the Born–Oppenheimer (BO) approximation are performed with extended Slater and Gaussian basis sets. In our computer code for nonorthogonal CI,[3] the integrals with Slater-type function (STF) functions are calculated by the SMILES code developed by Fernandez Rico *et al.*[4] Discussions on the basis sets and details of the techniques used to analyze the computed wave functions and energies, when common to the work in Refs. 1 and 2, are only summarized.

Experimentally,[5] a number of states have been assigned to $^3\Sigma_g^+$, specifically five states named a, g, h, p, and q with equilibrium total energies of −0.737 358, −0.660 273, (−0.660 006), −0.634 505, and −0.621 815 hartree, respectively (value within parentheses is uncertain[3]). For $^3\Sigma_u^+$, the lowest state (designated as the b state) is reported[5] as unstable; for the four stable states, named e, f, m, and t, the equilibrium total energies are −0.683 418, (−0.642 728), (−0.630 827), and (−0.621 828) hartree, respectively.

For early theoretical discussions on H_2 excited states, we recall the classical work by Herzberg[6] and Mulliken[7] among the many references given in Refs. 1 and 2. A few triplet states for the two Σ manifolds in H_2 have been accurately computed. For $^3\Sigma_g^+$ states, the most accurate PECs are the James-Coolidge-type CI computations in confocal elliptic coordinates[8] by Staszewska and Wolniewicz[9] for the three lowest states and those for the fourth and fifth excited states reported by Kolos and Rychlewski.[10] Nearly accurate computations for the first eight states using generalized Gaussian functions have been published by Detmer *et al.*,[11] where, however, most PECs are reported only graphically. Accurate computations limited to a few internuclear distances (for the second to fifth excited states) have been published by Liu and Hagstrom[12] using confocal elliptic basis orbitals and nonorthogonal CI.

For the $^3\Sigma_u^+$ states, the most accurate PEC computations are again those of James-Coolidge type by Staszewska and Wolniewicz[9] for the three lowest states and the nearly accurate computations for the lowest eight states by Detmer *et al.*[11] Accurate computations for the second and third states, limited however to eight internuclear distances, are reported

a)Electronic mail: corongiu@uninsubria.it.

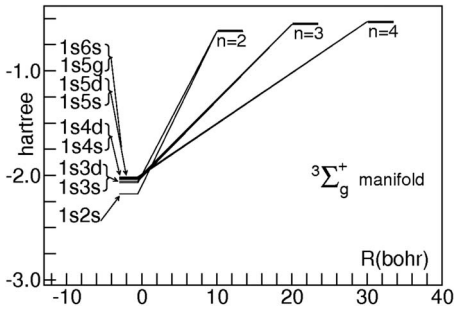

FIG. 1. Orbital correlation diagram for the $^3\Sigma_g^+$ states.

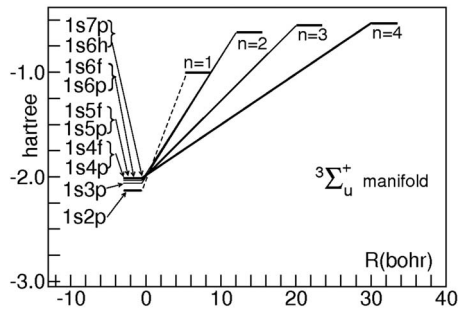

FIG. 2. Orbital correlation diagram for the $^3\Sigma_u^+$ states.

by Liu and Hagstrom.[12] The Hylleraas CI technique has been used by Preiskorn *et al.*[13] to compute the PECs for the second and third states.

In this work, all triplet states arising from the configurations $(1s^1nl^1)$ with n up to 5 and l up to 4, thus 14 states in total for $^3\Sigma_g^+$ and 15 states in total for $^3\Sigma_u^+$, are considered. Those with $n=5$ have the energy minimum close to the energy of the H_2^+ ion but well below the H(1s)+H(5l) dissociation limit. In the following, we shall designate the states not by the spectroscopic nomenclature but with numbers 1–15. With our nonorthogonal CI code,[3] we obtain, for a given symmetry, all the needed roots, ground, and excited states directly by diagonalization; therefore the state order is assigned unambiguously.

In this, as in preceding computations on H_2,[1,2] we do not aim at accurate benchmark computations. Our initial aim is to present at first systematic BO energy computations for H_2 excited states, which are energetically close to the most accurate BO computations in the literature. Furthermore, we are addressing a number of symmetries, and for each one we consider all the excited states dissociating from $H[^2S(1s^1)]+H[^2S(1s^1)]$ to $H[^2S(1s^1)]+H[^2X(nl^1)]$ with $n=1-5$ and $l=0-4$. Finally, our computed internuclear distances extend from the united atom up to full dissociation (10 000 bohrs) and are supplemented by a detailed analysis of the evolution of the electronic density at the different internuclear separations we have considered. Extension of these computations to different symmetries is in progress, and the inclusion of adiabatic corrections is our next computational step. Our computations differ from the accurate data by Staszewska and Wolniewicz[9] and Kołos and Rychlewski[10] from a maximum of 0.03 to about 0.00 kcal/mol, and at the equilibrium position the average deviation is 0.006 kcal/mol; thus our computations, even if not "accurate," are "realistic" enough for the aims of our work.

In Figs. 1 and 2 we report state orbital diagrams for the $^3\Sigma_g^+$ and $^3\Sigma_u^+$ states, respectively. These provide the electronic configurations for the triplet states at the united atom (He) and at dissociation for the H_2 molecule up to $n=4$, i.e., H(1s)+H(4l). In Figs. 1 and 2, starting from the left, the *total atomic* excited state energies of the united atom (with the corresponding atomic state configurations) are linearly connected (idealized molecular excited states) to the H_2 dissociation products, H(1s) and H(nl), indicated on the right side of the figures with the shorthand notation $n=1-4$. The $n=5$ states are not reported in the figures for reasons of space, but our computations do include the states dissociating with $n=5$ and l from 0 to 4, as well as the corresponding united atom states above $He[^3S(1s6s)]$.

For the $^3\Sigma_g^+$ manifold (Fig. 1), there is no state dissociating as $n=1$ due to the antisymmetry requirement of the wave function. In Fig. 2, which deals with the $^3\Sigma_u^+$ manifold, the first state, which at the united atom is $He[^3P(1s2p)]$ and dissociates as $n=1$, is indicated with a dashed line since it is unstable. In the figure the l value varies from 0 to 3 (i.e., from s to f orbitals), corresponding to the excited states up to $n=4$, namely, states 1–10.

Computationally, the high Σ states dissociating with $n=5$ require very extended basis sets capable of describing the configurations $(1s^16d^1)$ up to $(1s^18h^1)$ in the united atom and the H_2 dissociations H(1s)+H(5l), with l from 0 to 4. In addition, in these states there are many nodes and state crossings, making the corresponding computations somewhat demanding. Further, the PECs for states dissociating from H(1s)+H(1s) up to H(1s)+H(4l) are somewhat more accurately computed than the PECs for the states dissociating into H(1s)+H(5l) since the latter would benefit from the addition of the basis functions needed to describe states dissociating with $n>5$. For this reason, states dissociating as H(1s)+H(5l) are analyzed somewhat more briefly.

II. COMPUTED PECS

The computations of the PECs for the $^3\Sigma_g^+$ and $^3\Sigma_u^+$ states start with the united atom and end at a molecular internuclear distance of 10^4 bohrs. Two extended basis sets are used in this study: one constructed from STFs and the second from spherical Gaussian Type Functions (GTF). Note that we have used the notation STF and GTF, rather than the more usual Slater Type Orbital (STO) and Gaussian Type Orbital (GTO), to recall that the basis set is made up of analytical functions and not necessarily of orbitals. The two optimized basis sets, Slater and Gaussian, are nearly equivalent, and the computations obtained with the two types of functions yield only slightly different eigenvalues (and correspondingly only slightly different electronic densities) for a given internuclear separation. The use of two different basis functions provides a useful numerical check on the computational accuracy and adds flexibility to the interpretation of the computations, as discussed in detail in Refs. 1 and 2.

The hydrogen STF basis set is made up of two 1s, three 2s, two 3s, two 4s, one 5s, four 2p, two 3p, two 4p, two 5p, four 3d, one 4d, two 5d, three 4f, three 5f, and one 5g func-

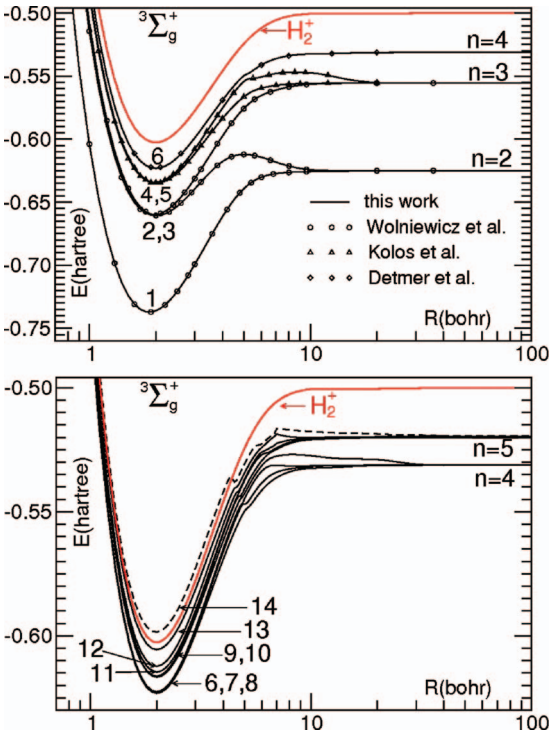

FIG. 3. $^3\Sigma_g^+$ manifold: PECs for states 1–13 (full lines) for ground state of H_2^+ (red line) and for state 14 (dashed line; see text).

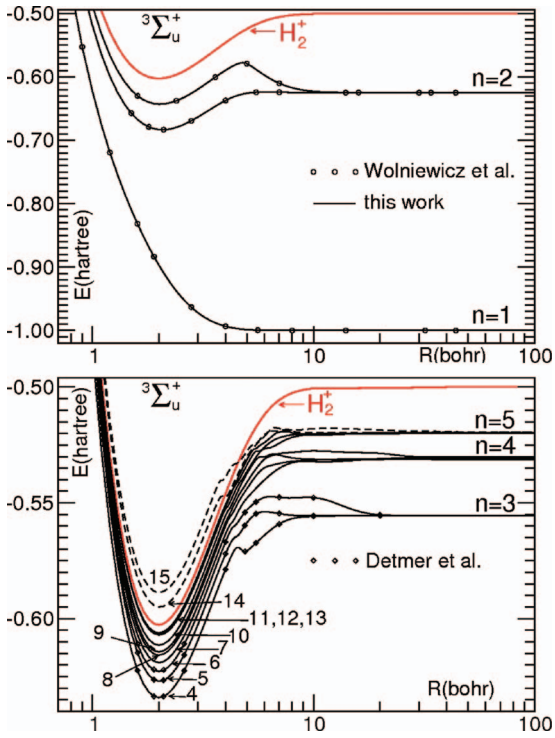

FIG. 4. $^3\Sigma_u^+$ manifold: PECs for states 1–13 (full line) for ground state of H_2^+ (red line) and for states 14 and 15 (dashed lines; see text).

tions. The GTF basis set is made up of 18s, 11p, 12d, 7f, and 1g contracted to 13s, 11p, 9d, 5f, and 1g functions. In the united atom, the helium basis set is formed by three 1s, three 2s, two 3s, two 4s, one 5s, two 6s, one 7s, one 8s, four 2p, two 3p, two 4p, two 5p, one 6p, one 7p, one 8p, four 3d, one 4d, two 5d, one 6d, one 7d one 8d, four 4f, three 5f, one 6f, two 7f, two 8f functions and one function each for 5g, 6g, 6h, and 7h.

The H_2 dissociation products are well represented by the above STF basis set, which accurately reproduces hydrogenic functions; for additional details on the hydrogenic functions for H_2, see Ref. 1. Also, the helium energies for the excited states (singlet and triplet) with configuration (1s1s) up to (1s8f) are nicely reproduced (but somewhat less accurately for the higher energy states). Note that the present basis set extension, relative to Refs. 1 and 2, has made the computations of the states dissociating with $n=5$ somewhat more accurate than those reported previously.[1,2]

In Fig. 3, we report the computed PECs for the $^3\Sigma_g^+$ states 1–14; in Fig. 4 equivalent data are reported for the $^3\Sigma_u^+$ states 1–15. The internuclear separations considered are 117, precisely 15 from 0.01–0.9 bohr and 100 from 1.0–100 bohrs; computations at 1000 and 10 000 bohrs are performed to define the dissociation products.

In Fig. 3, the top inset reports the PECs of the first six $^3\Sigma_g^+$ states. In this figure the small circles, the triangles, and the diamonds selectively sample the energies from the data of Staszewska and Wolniewicz,[9] Kolos and Rychlewski,[10] and Detmer *et al.*,[11] respectively. In the bottom inset, the $^3\Sigma_g^+$ PECs for the states 6–13 are reported as full lines, for state 14 (with equilibrium energy above that of H_2^+) as dashed line. In the figure, we have included the PEC for the ground state of H_2^+ (red color).

In Fig. 4, the top inset reports the $^3\Sigma_u^+$ PECs of the first three states. In this figure, the small circles represent a selected sample of energies from the data of Staszewska and Wolniewicz.[9] In the bottom inset, the $^3\Sigma_u^+$ PECs for states 4–13 are reported as a full line; small diamonds are used to represent the energies from Detmer *et al.*[11] In addition, we report the ground state energies for H_2^+ (red color) and the PECs for states 14 and 15 (dashed line), the latter with equilibrium energy above that of H_2^+. The energy scale used in Fig. 4 does not allow to see in state 1 the van der Waals very shallow minimum at about 7.8 bohrs; its computed energy is $-1.000\,019\,8$ hartree, compared to $-1.000\,020\,5$ hartree by Staszewska and Wolniewicz,[9] i.e., a difference of 0.17 cm^{-1}.

From Figs. 3 and 4, it is apparent that the energies from this work are in good agreement with those computed by Staszewska and Wolniewicz,[9] Kolos and Rychlewski,[10] and Detmer *et al.*,[11] taken as reference data. Specifically, we report on energy differences between our data and the reference data; the difference is a positive value when the reference is lower in energy and negative when our energy is lower. For the $^3\Sigma_g^+$ manifold, the average deviation (in hartree) from Staszewska and Wolniewicz[9] for states 1–3 are 1.3×10^{-5} (with maximum deviation of 3.0×10^{-5} at 4.2 bohrs), 1.8×10^{-5} (with maximum deviation of 4.1×10^{-5} at 6.4 bohrs), and 1.3×10^{-5} (with maximum deviation of 2.4×10^{-5} at 6.8 bohrs). For the same manifold, the average deviation (in hartree) from Kolos and Rychlewski[10] for states 4 and 5 are 7.1×10^{-6} (with maximum deviation of -2.0×10^{-5} at 1.1 bohrs) and 1.5×10^{-5} (with maximum deviation of -4.6×10^{-5} at 15 bohrs), respectively; finally the average deviation (in hartree) from Detmer *et al.*[11] for state 6 is -2.2×10^{-4}, with our data lower than those in Ref. 11.

TABLE I. $^3\Sigma_g^+$ manifold. Comparison of our computed energies (hartree) near the equilibrium separation with those of Staszewska *et al.* (Ref. 9), Kolos *et al.* (Ref. 10), Detmer *et al.* (Ref. 11), and Liu *et al.* (Ref. 12) designated as S, K, D, and L, respectively.

State	R (bohr)	S, K,andD	This work	L
1	1.9	−0.737 090 (S)	−0.737 080	⋯
2	2.0	−0.660 568 (S)	−0.660 562	−0.660 566
3	2.0	−0.659 842 (S)	−0.659 833	−0.659 840
4	2.0	−0.634 917(K)	−0.634 915	−0.634 920
5	2.0	−0.634 507(K)	−0.634 483	−0.634 509
6	2.0	−0.622 769(D)	−0.623 163	⋯

Table I compares the $^3\Sigma_g^+$ energies near the equilibrium distance computed by Staszewska and Wolniewicz,[9] Kolos and Rychlewski,[10] and Detmer *et al.*[11] (second column with identifications S, K, and D, respectively) with our computed energies (third column); the Liu *et al.*[12] data are given in the fourth column. Recall that the computed energies of the H_2^+ ion for the $^2\Sigma_g^+(1\sigma_g)$ and $^2\Sigma_u^+(1\sigma_u)$ states (obtained with the same basis set used in this work) at 2.0 bohrs are −0.602 633 and −0.167 533 hartree, respectively; these values differ by 1.5×10^{-6} hartree from the best results in Ref. 14.

For the $^3\Sigma_u^+$ manifold, the average deviations (in hartree) from Staszewska and Wolniewicz[9] for states 1–3 are 1.1×10^{-5} (with maximum deviation of 4.6×10^{-5} at 0.2 bohr), 7.0×10^{-6} (with maximum deviation of 1.9×10^{-5} at 4.1 bohrs), and 1.5×10^{-5} (with maximum deviation of 5.9×10^{-5} at 6.8 bohrs). For the same manifold the average deviation (in hartree) from Detmer *et al.*[11] for states 4–6 are 1.9×10^{-6} and -4.4×10^{-5} at 4.0 bohrs, -1.3×10^{-5}, and -1.0×10^{-4}. Thus, some energies are slightly less and others are slightly more accurately computed than those in Ref. 11.

Table II compares the $^3\Sigma_u^+$ energies, near the equilibrium distance, computed by Staszewska and Wolniewicz[9] and Detmer *et al.*[11] (second column with identifications S and D, respectively) with our computed energies (third column). Tables I and II document the good quality of the computations presented in this work.

In Tables III and IV, we present a tabulation of the computed energies at selected internuclear separations of the 12 lowest states both for the $^3\Sigma_g^+$ and $^3\Sigma_u^+$ states. Note that from R=0 to R=0.6 bohr, we have reported the electronic energy, thereafter the total energy.

TABLE II. $^3\Sigma_u^+$ manifold. Comparison of our computed energies (hartree) near equilibrium separation with those of Staszewska *et al.* (Ref. 9) and Detmer *et al.* (Ref. 11), designated as S and D, respectively.

State	R (bohr)	S andD	This work
1[a]	2.0	−0.897 076 (S)	−0.897 059
2	2.1	−0.683 420 (S)	−0.683 416
3[b]	2.0	−0.643 030 (S)	−0.643 028
4	2.0	−0.634 099(D)	−0.634 097
5	2.0	−0.627 014(D)	−0.627 022
6	2.0	−0.622 564(D)	−0.622 733

[a]State 1 is not bound.
[b]−0.643 027 hartree in Ref. 12.

For very short internuclear distances, from R=0.0 to R=0.9 bohr, we report the computed results in Figs. 5 and 6. The PECs in these figures correspond to *electronic* rather than *total* energies. In each figure the PECs merge smoothly into the corresponding helium excited state energies; therefore proposals for adopting a linear interpolation from R=1.0 to R=0 bohr appear somewhat crude, as noted previously.[1,2]

From R=0.01 to 0.07 bohr the PECs are obtained from computations with the helium STF basis set centered midway the two hydrogen nuclei. For the inter-nuclear distances from 0.8 to 0.9 bohr we report CI computed energies obtained with STF centered on two H atoms. In the figures we have indicated with a short vertical bar the inter-nuclear separation at 0.08 bohr. For PECs of states higher than 10, the small energy discontinuity shown between 0.07 and 0.08 bohr is due to different computational techniques with non-equivalent basis sets. Further, the two electrons merge into an atomic structure at inter-nuclear distances larger than those of the two H nuclei merging into the helium nucleus. As one can appreciate from Figs. 5 and 6, the change of computational technique at very short distances does not change the overall conclusion: the PECs smoothly, and not linearly, merge into the united atom.

In conclusion the PECs reported in this work are very close to the best computations in the literature for the H_2 molecule and are thus appropriate for the main task of this work. Inspection of Figs. 3 and 4 calls for comments on the bumps and crossings in the region of 4–6 bohrs, leading to apparent "irregular" features. This subject is discussed in detail by Mulliken;[7] however, his conclusions are obtained without the availability of accurate energies for the high energy states, which are essential to fully characterize the two sigma triplet state manifolds.

The pattern of states in each one of the two manifolds suggests a "first" system of excited states with the principal minimum around 2 bohrs interacting with a "second" system of states leading to barriers, bumps, and "virtual" double minimum states. The first set of minima is evident by inspection of Figs. 2 and 3. The interaction of the first set of states with the second high energy system is responsible for the PEC barriers and bumps. For example, in the $^3\Sigma_g^+$ manifold, note the barriers in states 2 and 5–10 after the internuclear distance of 4 bohrs. For the $^3\Sigma_u^+$ manifold, note the bumps for states 3–14. Note in addition the crossings for the $^3\Sigma_g^+$ manifold, immediately before the equilibrium distance, between states 2 and 3, 4 and 5, and the very close energies for the three states 11–13.

III. DECOMPOSITION INTO IONIC AND COVALENT COMPONENTS

The full CI of HL orbitals leads to the decomposition of the total state energies into ionic and covalent components (see for details Ref. 1). For the $^1\Sigma_g^+$ and $^1\Sigma_u^+$ states, it is found that each manifold dissociating at a specific n value [namely,

TABLE III. Energy values (hartree) at internuclear distances R (bohr) for $^3\Sigma_g^+$ states 1–12.

	R										
State	**0.00**	**0.08**	**0.10**	**0.20**	**0.40**	**0.60**	**0.80**	**1.00**	**1.20**	**1.40**	**1.60**
1	−2.175 21	−2.160 16	−2.152 63	−2.101 12	−1.968 25	−1.833 61	−0.461 42	−0.603 91	−0.676 67	−0.713 63	−0.730 88
2	−2.068 68	−2.054 03	−2.046 70	−1.996 59	−1.867 46	−1.736 80	−0.368 43	−0.514 44	−0.590 42	−0.630 30	−0.650 22
3	−2.055 63	−2.041 11	−2.033 86	−1.984 23	−1.856 45	−1.727 29	−0.360 42	−0.507 90	−0.585 30	−0.626 57	−0.647 83
4	−2.036 51	−2.021 92	−2.014 63	−1.964 81	−1.836 46	−1.706 64	−0.339 09	−0.485 88	−0.562 57	−0.603 12	−0.623 65
5	−2.031 28	−2.016 75	−2.009 50	−1.959 86	−1.832 05	−1.702 83	−0.335 89	−0.483 27	−0.560 56	−0.601 68	−0.622 77
6	−2.022 62	−2.007 99	−2.000 72	−1.950 98	−1.822 89	−1.693 35	−0.326 07	−0.473 12	−0.550 06	−0.590 84	−0.611 60
7	−2.020 01	−2.005 44	−1.998 18	−1.948 55	−1.820 72	−1.691 48	−0.324 51	−0.471 86	−0.549 10	−0.590 16	−0.611 18
8	−2.020 00	−2.005 35	−1.998 10	−1.948 46	−1.820 61	−1.691 36	−0.324 36	−0.471 67	−0.548 86	−0.589 88	−0.610 84
9	−2.015 25	−2.000 65	−1.993 39	−1.943 69	−1.815 67	−1.686 23	−0.319 05	−0.466 18	−0.543 20	−0.584 06	−0.604 90
10	−2.013 80	−1.999 15	−1.991 90	−1.942 26	−1.814 43	−1.685 18	−0.318 21	−0.465 54	−0.542 76	−0.583 81	−0.604 79
11	−2.011 55	−1.997 39	−1.990 13	−1.940 49	−1.812 64	−1.683 38	−0.316 39	−0.463 70	−0.540 90	−0.581 92	−0.602 90
12	−2.010 99	−1.996 45	−1.989 19	−1.939 51	−1.811 55	−1.682 16	−0.315 02	−0.462 19	−0.539 23	−0.580 09	−0.600 90
	1.70	**1.90**	**2.00**	**2.10**	**2.20**	**2.40**	**2.50**	**2.70**	**3.00**	**3.30**	**3.60**
1	−0.734 91	−0.737 08	−0.736 10	−0.734 15	−0.731 47	−0.724 61	−0.720 68	−0.712 28	−0.699 26	−0.686 63	−0.675 00
2	−0.655 49	−0.660 10	−0.660 56	−0.660 24	−0.659 21	−0.655 56	−0.653 20	−0.647 90	−0.639 45	−0.631 44	−0.624 59
3	−0.653 75	−0.659 44	−0.659 83	−0.658 99	−0.657 30	−0.652 26	−0.649 16	−0.642 31	−0.631 28	−0.620 30	−0.609 96
4	−0.629 22	−0.634 36	−0.634 92	−0.634 51	−0.633 33	−0.629 33	−0.626 76	−0.620 97	−0.611 57	−0.602 26	−0.593 65
5	−0.628 59	−0.634 07	−0.634 48	−0.633 83	−0.632 36	−0.627 76	−0.624 87	−0.618 41	−0.607 91	−0.597 38	−0.587 41
6	−0.617 27	−0.622 61	−0.623 16	−0.622 71	−0.621 47	−0.617 33	−0.614 69	−0.608 71	−0.598 97	−0.589 23	−0.580 07
7	−0.616 96	−0.622 34	−0.622 81	−0.622 23	−0.620 86	−0.616 51	−0.613 78	−0.607 63	−0.597 55	−0.587 40	−0.577 75
8	−0.616 61	−0.622 02	−0.622 56	−0.622 06	−0.620 77	−0.616 40	−0.613 60	−0.607 29	−0.596 99	−0.586 64	−0.576 81
9	−0.610 65	−0.616 11	−0.616 67	−0.616 21	−0.614 96	−0.610 78	−0.608 10	−0.602 06	−0.592 18	−0.582 26	−0.572 88
10	−0.610 52	−0.615 82	−0.616 29	−0.615 74	−0.614 39	−0.610 00	−0.607 22	−0.600 96	−0.590 75	−0.580 47	−0.570 71
11	−0.608 67	−0.614 10	−0.614 64	−0.614 15	−0.612 87	−0.608 61	−0.605 89	−0.599 76	−0.589 71	−0.579 58	−0.569 95
12	−0.606 59	−0.611 86	−0.612 32	−0.611 75	−0.610 39	−0.605 98	−0.603 19	−0.596 92	−0.586 69	−0.576 44	−0.566 75
	4.00	**4.40**	**4.80**	**5.20**	**5.60**	**5.80**	**6.20**	**6.60**	**7.00**	**7.60**	**8.00**
1	−0.661 54	−0.650 71	−0.642 49	−0.636 65	−0.632 73	−0.631 33	−0.629 35	−0.628 11	−0.627 34	−0.626 65	−0.626 36
2	−0.617 85	−0.613 93	−0.612 29	−0.612 19	−0.613 03	−0.613 65	−0.615 13	−0.616 72	−0.618 27	−0.620 27	−0.621 36
3	−0.597 67	−0.587 37	−0.579 14	−0.572 88	−0.568 39	−0.566 72	−0.564 22	−0.562 45	−0.561 08	−0.559 46	−0.558 61
4	−0.583 68	−0.575 52	−0.569 08	−0.564 33	−0.561 31	−0.560 33	−0.558 98	−0.558 02	−0.557 35	−0.556 68	−0.556 40
5	−0.575 50	−0.565 45	−0.557 42	−0.552 45	−0.551 67	−0.551 26	−0.550 03	−0.548 84	−0.547 98	−0.547 27	−0.547 06
6	−0.569 21	−0.560 05	−0.552 63	−0.548 20	−0.544 64	−0.542 82	−0.539 85	−0.537 72	−0.536 18	−0.534 61	−0.533 88
7	−0.566 18	−0.556 33	−0.548 23	−0.545 87	−0.541 59	−0.539 79	−0.537 01	−0.535 17	−0.534 05	−0.533 10	−0.532 73
8	−0.565 04	−0.555 08	−0.547 55	−0.541 79	−0.536 90	−0.535 02	−0.532 44	−0.531 39	−0.531 32	−0.531 47	−0.531 53
9	−0.561 66	−0.552 14	−0.544 69	−0.539 85	−0.534 92	−0.532 94	−0.529 95	−0.528 28	−0.527 58	−0.527 08	−0.526 96
10	−0.559 02	−0.549 11	−0.543 65	−0.537 88	−0.532 99	−0.531 01	−0.527 92	−0.525 96	−0.524 74	−0.523 22	−0.522 48
11	−0.558 41	−0.548 60	−0.540 77	−0.534 43	−0.529 74	−0.528 08	−0.526 38	−0.525 61	−0.524 26	−0.522 70	−0.521 98
12	−0.555 27	−0.545 73	−0.540 27	−0.533 90	−0.528 93	−0.527 08	−0.525 33	−0.524 01	−0.522 42	−0.521 52	−0.521 12
	8.50	**9.00**	**9.50**	**10.00**	**11.00**	**12.00**	**15.00**	**20.00**	**30.00**	**50.00**	**100**
1	−0.626 12	−0.625 96	−0.625 84	−0.625 76	−0.625 65	−0.625 56	−0.625 34	−0.625 14	−0.625 04	−0.625 01	−0.625 00
2	−0.622 45	−0.623 26	−0.623 85	−0.624 26	−0.624 72	−0.624 91	−0.625 01	−0.625 00	−0.625 00	−0.625 00	−0.625 00
3	−0.557 77	−0.557 16	−0.556 71	−0.556 39	−0.556 01	−0.555 82	−0.555 63	−0.555 58	−0.555 56	−0.555 56	−0.555 56
4	−0.556 16	−0.556 00	−0.555 89	−0.555 82	−0.555 72	−0.555 66	−0.555 58	−0.555 56	−0.555 56	−0.555 56	−0.555 55
5	−0.546 98	−0.547 02	−0.547 17	−0.547 42	−0.548 24	−0.549 40	−0.552 90	−0.555 21	−0.555 54	−0.555 54	−0.555 54
6	−0.533 24	−0.532 82	−0.532 58	−0.532 45	−0.532 32	−0.532 22	−0.531 76	−0.531 34	−0.531 25	−0.531 25	−0.531 25
7	−0.532 39	−0.532 13	−0.531 92	−0.531 74	−0.531 51	−0.531 40	−0.531 28	−0.531 25	−0.531 23	−0.531 24	−0.531 23
8	−0.531 56	−0.531 55	−0.531 51	−0.531 47	−0.531 40	−0.531 35	−0.531 27	−0.531 24	−0.531 20	−0.531 23	−0.531 22
9	−0.526 96	−0.527 06	−0.527 22	−0.527 41	−0.527 83	−0.528 21	−0.528 71	−0.528 94	−0.530 84	−0.531 18	−0.531 18
10	−0.521 81	−0.521 36	−0.521 08	−0.520 91	−0.520 72	−0.520 60	−0.520 28	−0.520 19	−0.520 05	−0.520 00	−0.520 00
11	−0.521 37	−0.520 94	−0.520 64	−0.520 43	−0.520 20	−0.520 15	−0.520 09	−0.520 00	−0.519 95	−0.519 93	−0.519 94
12	−0.520 78	−0.520 55	−0.520 40	−0.520 30	−0.520 19	−0.520 10	−0.520 02	−0.519 92	−0.519 75	−0.519 86	−0.519 76

with dissociation products $H(1s)+H(nl)$] contains at least one state with a finite contribution of the ionic energy component.

Denoting the total energy as E_{tot} and the covalent energy component as E_{cov}, we have defined[1,2] the ionic energy percent $(IEP)=100(1-\eta)$, where $\eta=E_{cov}/E_{tot}$. This covalent-ionic decomposition, when applied to the $^3\Sigma_g^+$ and $^3\Sigma_u^+$ manifolds, leads to the conclusion that most triplet sigma states

TABLE IV. Energy values (hartree) at internuclear distances R (bohr) for $^3\Sigma_u^+$ states 1–12.

	R										
State	**0.00**	**0.08**	**0.10**	**0.20**	**0.40**	**0.60**	**0.80**	**1.00**	**1.20**	**1.40**	**1.60**
1	−2.133 13	−2.118 89	−2.111 77	−2.063 19	−1.939 29	−1.816 75	−0.460 08	−0.622 25	−0.719 22	−0.784 23	−0.831 74
2	−2.058 07	−2.043 63	−2.036 41	−1.987 08	−1.860 33	−1.732 85	−0.368 33	−0.518 72	−0.599 29	−0.643 55	−0.667 32
3	−2.032 31	−2.017 83	−2.010 59	−1.961 07	−1.833 68	−1.705 13	−0.339 10	−0.487 57	−0.565 98	−0.608 11	−0.630 01
4	−2.031 25	−2.016 73	−2.009 47	−1.959 83	−1.831 99	−1.702 75	−0.335 76	−0.483 09	−0.560 30	−0.601 34	−0.622 32
5	−2.020 54	−2.006 04	−1.998 79	−1.949 22	−1.821 60	−1.692 69	−0.326 17	−0.474 04	−0.551 80	−0.593 34	−0.614 73
6	−2.020 00	−2.005 46	−1.998 21	−1.948 57	−1.820 73	−1.691 47	−0.324 48	−0.471 80	−0.549 00	−0.590 02	−0.610 99
7	−2.014 20	−1.999 69	−1.992 44	−1.942 84	−1.815 12	−1.686 06	−0.319 33	−0.466 95	−0.544 46	−0.585 76	−0.606 95
8	−2.013 80	−1.998 47	−1.991 22	−1.941 59	−1.813 75	−1.684 50	−0.317 51	−0.464 83	−0.542 03	−0.583 05	−0.604 03
9	−2.013 79	−1.995 87	−1.988 61	−1.939 00	−1.811 23	−1.682 10	−0.315 27	−0.462 77	−0.540 15	−0.581 34	−0.602 44
10	−2.010 15	−1.993 09	−1.985 83	−1.936 22	−1.808 47	−1.679 35	−0.312 52	−0.460 01	−0.537 37	−0.578 52	−0.599 58
11	−2.010 09	−1.989 30	−1.982 04	−1.932 40	−1.804 56	−1.675 31	−0.308 32	−0.455 65	−0.532 87	−0.573 93	−0.594 95
12	−2.009 44	−1.988 80	−1.981 56	−1.931 98	−1.804 18	−1.674 93	−0.307 94	−0.455 27	−0.532 47	−0.573 63	−0.594 92
	1.70	**1.90**	**2.00**	**2.10**	**2.20**	**2.40**	**2.50**	**2.70**	**3.00**	**3.30**	**3.60**
1	−0.851 14	−0.883 52	−0.897 06	−0.909 12	−0.919 85	−0.937 89	−0.945 43	−0.958 04	−0.971 99	−0.981 53	−0.987 98
2	−0.674 29	−0.681 76	−0.683 15	−0.683 42	−0.682 81	−0.679 70	−0.677 48	−0.672 24	−0.663 41	−0.654 53	−0.646 36
3	−0.636 17	−0.642 23	−0.643 03	−0.642 76	−0.641 67	−0.637 73	−0.635 15	−0.629 23	−0.619 47	−0.609 65	−0.600 42
4	−0.628 10	−0.633 55	−0.634 10	−0.633 62	−0.632 35	−0.628 12	−0.625 42	−0.619 32	−0.609 35	−0.599 34	−0.589 88
5	−0.620 67	−0.626 37	−0.627 02	−0.626 63	−0.625 42	−0.621 28	−0.618 62	−0.612 56	−0.602 60	−0.592 58	−0.583 12
6	−0.616 76	−0.622 19	−0.622 73	−0.622 25	−0.620 96	−0.616 71	−0.613 99	−0.607 86	−0.597 84	−0.587 75	−0.578 20
7	−0.612 81	−0.618 38	−0.618 97	−0.618 52	−0.617 28	−0.613 07	−0.610 37	−0.604 26	−0.594 24	−0.584 14	−0.574 59
8	−0.609 79	−0.615 22	−0.615 76	−0.615 27	−0.613 99	−0.609 73	−0.607 01	−0.600 88	−0.590 84	−0.580 73	−0.571 17
9	−0.608 26	−0.613 76	−0.614 33	−0.613 86	−0.612 60	−0.608 36	−0.605 65	−0.599 51	−0.589 46	−0.579 33	−0.569 74
10	−0.605 38	−0.610 86	−0.611 42	−0.610 94	−0.609 67	−0.605 41	−0.602 69	−0.596 55	−0.586 48	−0.576 34	−0.566 72
11	−0.600 81	−0.606 42	−0.607 03	−0.606 60	−0.605 36	−0.601 17	−0.598 47	−0.592 37	−0.582 46	−0.572 56	−0.563 18
12	−0.600 73	−0.606 24	−0.606 81	−0.606 37	−0.605 14	−0.600 98	−0.598 31	−0.592 30	−0.582 36	−0.572 28	−0.562 78
	4.00	**4.40**	**4.80**	**5.20**	**5.60**	**5.80**	**6.20**	**6.60**	**7.00**	**7.60**	**8.00**
1	−0.993 36	−0.996 42	−0.998 13	−0.999 06	−0.999 55	−0.999 70	−0.999 88	−0.999 96	−1.000 00	−1.000 02	−1.000 02
2	−0.637 34	−0.630 93	−0.627 03	−0.625 06	−0.624 25	−0.624 09	−0.624 01	−0.624 09	−0.624 21	−0.624 38	−0.624 48
3	−0.589 74	−0.581 55	−0.577 50	−0.582 65	−0.590 35	−0.594 00	−0.600 48	−0.605 82	−0.610 13	−0.614 92	−0.617 25
4	−0.578 74	−0.570 23	−0.570 73	−0.569 45	−0.566 60	−0.565 25	−0.562 79	−0.560 73	−0.559 12	−0.557 46	−0.556 79
5	−0.572 09	−0.564 94	−0.561 10	−0.556 60	−0.554 38	−0.553 96	−0.553 87	−0.554 22	−0.554 65	−0.555 16	−0.555 38
6	−0.566 90	−0.559 93	−0.555 13	−0.551 47	−0.549 05	−0.548 20	−0.547 37	−0.547 36	−0.547 64	−0.547 91	−0.547 90
7	−0.563 42	−0.556 74	−0.550 16	−0.546 16	−0.542 92	−0.541 46	−0.538 87	−0.536 73	−0.535 07	−0.533 36	−0.532 66
8	−0.559 88	−0.552 88	−0.546 38	−0.541 47	−0.537 35	−0.535 87	−0.534 24	−0.533 56	−0.533 02	−0.532 39	−0.532 15
9	−0.558 49	−0.550 23	−0.543 80	−0.538 59	−0.534 30	−0.532 55	−0.530 21	−0.529 32	−0.529 38	−0.530 19	−0.530 59
10	−0.555 44	−0.548 03	−0.540 45	−0.534 66	−0.530 64	−0.530 14	−0.529 72	−0.528 92	−0.528 72	−0.528 36	−0.528 20
11	−0.552 61	−0.545 29	−0.539 30	−0.533 77	−0.529 18	−0.527 44	−0.526 35	−0.525 61	−0.524 25	−0.522 52	−0.521 75
12	−0.551 94	−0.542 82	−0.536 83	−0.530 69	−0.527 65	−0.527 32	−0.524 76	−0.522 95	−0.521 98	−0.521 07	−0.520 72
	8.50	**9.00**	**9.50**	**10.00**	**11.00**	**12.00**	**15.00**	**20.00**	**30.00**	**50.00**	**100**
1	−1.000 02	−1.000 01	−1.000 01	−1.000 01	−1.000 00	−1.000 00	−1.000 00	−1.000 00	−1.000 00	−1.000 00	−1.000 00
2	−0.624 58	−0.624 66	−0.624 73	−0.624 79	−0.624 89	−0.624 95	−0.625 01	−0.625 00	−0.625 00	−0.625 00	−0.625 00
3	−0.619 43	−0.620 98	−0.622 09	−0.622 86	−0.623 79	−0.624 24	−0.624 68	−0.624 87	−0.624 96	−0.624 99	−0.625 00
4	−0.556 30	−0.556 04	−0.555 91	−0.555 84	−0.555 75	−0.555 69	−0.555 59	−0.555 56	−0.555 56	−0.555 56	−0.555 56
5	−0.555 54	−0.555 60	−0.555 61	−0.555 59	−0.555 56	−0.555 54	−0.555 54	−0.555 54	−0.555 55	−0.555 55	−0.555 55
6	−0.547 78	−0.547 65	−0.547 61	−0.547 70	−0.548 33	−0.549 40	−0.552 87	−0.555 20	−0.555 54	−0.555 54	−0.555 54
7	−0.532 22	−0.532 15	−0.532 19	−0.532 23	−0.532 26	−0.532 21	−0.531 75	−0.531 34	−0.531 25	−0.531 25	−0.531 25
8	−0.531 94	−0.531 70	−0.531 54	−0.531 44	−0.531 34	−0.531 31	−0.531 27	−0.531 25	−0.531 23	−0.531 24	−0.531 23
9	−0.530 91	−0.531 11	−0.531 21	−0.531 27	−0.531 31	−0.531 30	−0.531 25	−0.531 23	−0.531 20	−0.531 23	−0.531 22
10	−0.527 98	−0.527 79	−0.527 69	−0.527 68	−0.527 89	−0.528 21	−0.528 71	−0.528 94	−0.530 84	−0.531 18	−0.531 18
11	−0.521 13	−0.520 80	−0.520 69	−0.520 68	−0.520 68	−0.520 60	−0.520 28	−0.520 19	−0.520 05	−0.520 00	−0.520 00
12	−0.520 48	−0.520 35	−0.520 29	−0.520 28	−0.520 21	−0.520 16	−0.520 09	−0.519 99	−0.519 95	−0.519 93	−0.519 94

are covalent, particularly from the united atom to internuclear separations larger than the equilibrium energy, but a few states have a *small* ionic component (nearly ten times smaller than the singlet states[1,2]), which by lowering the energy in the covalent component enhances the eventual barriers present in the latter. However, we find no evidence that ionic configurations *originate* the barriers.[11,15]

In Fig. 7 we quantitatively report in the top insets the

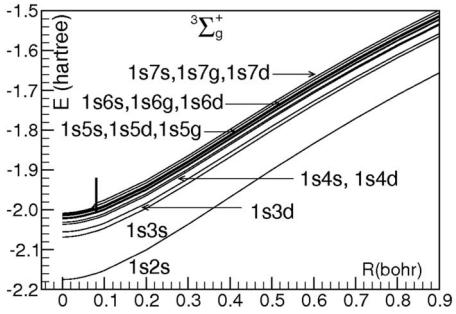

FIG. 5. Electronic energy curves for $^3\Sigma_g^+$ manifold from R=0 to R=0.9 bohr.

computed IEP for the states 2, 4, and 5 in the $^3\Sigma_g^+$ manifold and for the states 3–6 in the $^3\Sigma_u^+$ manifold; in the bottom insets we report the total energy (black) and the covalent energy component (red) for these states. Note that since the total and covalent component energies are very close (nearly superimposed in the figure), the intensity of the ionic character is always small and becomes essentially vanishing for the $^3\Sigma_g^+$ states 1, 3, and 6 and for the $^3\Sigma_u^+$ states 1 and 2 not reported in the figure. Concerning the nonsmooth and seemingly irregular behavior of the IEP intensity, for example, for state 5 in the $^3\Sigma_g^+$ manifold, first we recall that ionic character is related to the presence of ionic configurations. Further, as detailed in the density analysis (next two sections) along a given PEC, switches often occur among the dominant configuration functions. For example, in the $^3\Sigma_g^+$ manifold, the pattern of the IEP of state 5—characterized by three maxima—is explained by the variation from a 4d to a 4s to a 4p and to a 3d dominant character in the PEC wave function responsible for the nonsmooth pattern of the PEC, the latter reported in the bottom inset of the figure. Equivalently, in the $^3\Sigma_u^+$ manifold, the PEC of state 6 has 1s5f as the dominant configuration until about 4 bohrs, 1s3p around 5 bohrs, 1s3d at 6 bohrs, and then an ionic configuration starting at around 10 bohrs. Thus, we conclude that the IEP is locally very sensitive to electronic density in the wave function.

For high energy states, the decomposition into covalent and ionic states is complicated by the known fact that the full CI from HL orbitals yields both the *g* and *u* states, mixed together but ordered by increasing energy; thus state-by-state symmetry identification is required before proceeding with the decomposition. Unfortunately, the higher the state, the more difficult the identification becomes since the diagonal-

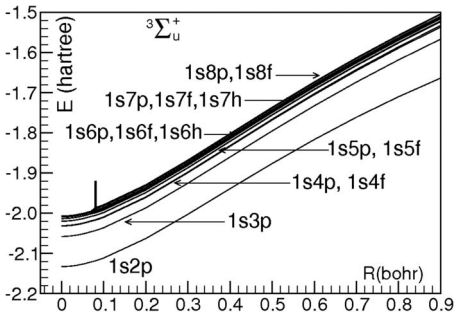

FIG. 6. Electronic energy curves for $^3\Sigma_u^+$ manifold from R=0 to R=0.9 bohr.

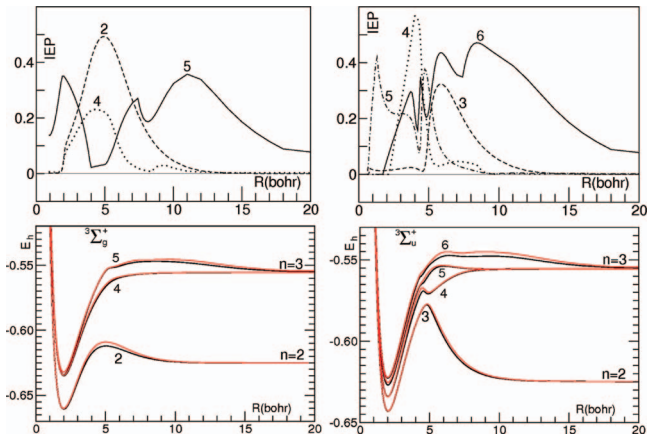

FIG. 7. Ionic percent energy. Top insets: for states 2 4 and 5 in the $^3\Sigma_g^+$ manifold and for states 3–6 in the $^3\Sigma_u^+$ manifold. Bottom: total energy (black) and covalent energy component (red) for the states in the top insets.

ization roots are more and more nearly degenerate; for several of the high energy states, a weakly ionic character is present but not quantitatively documented in this work. We conclude that ionic character in the H_2 molecule is a characteristic not only of the singlet sigma state manifolds but also of triplet state manifolds.

IV. ANALYSIS OF THE $^3\Sigma_g^+$ manifold

Mulliken in his classical 1966 analysis[7] subdivided the Rydberg states of H_2 into two classes, one dissociating smoothly along a normal potential curve and the other dissociating along a curve with eventual humps due to interactions between configurations. His analysis is based on the few accurate or nearly accurate H_2 wave functions for low excited states available to him at the time (particularly Refs. 16–19) and on a vast repertoire of spectroscopic data for diatomic molecules interpreted basically in the Linear Combination of Atomic Orbital-Molecular Orbital (LCAO-MO) approximation with limited configuration mixing corrections most often assumed rather than obtained from direct computations. In this context, we mention the pioneering work by Rothenberg *et al.*[20] on the lowest and on a few low excited states at five H_2 internuclear separations; note that the reported energies are somewhat less accurate than those in Refs. 9 and 10 or in our work. The analysis of Rothenberg *et al.*[20] of the wave function with Löwdin natural orbitals[21] cannot be easily compared with computations performed with either the STF or GTF basis sets, which are the most commonly used functions in contemporary molecular computations.

About half a century later, we have available for our analysis of H_2 realistic wave functions for 29 excited states both for the singlet and triplet sigma states, starting from the united atom up to full dissociation. Furthermore, the use of full CI of Heitler–London type allows a quantitative discussion of the ionic component of the total state energies. In this work we limit the discussion to Σ states; a study of the manifolds of states with Π, Δ, and Φ symmetries is in progress.[22]

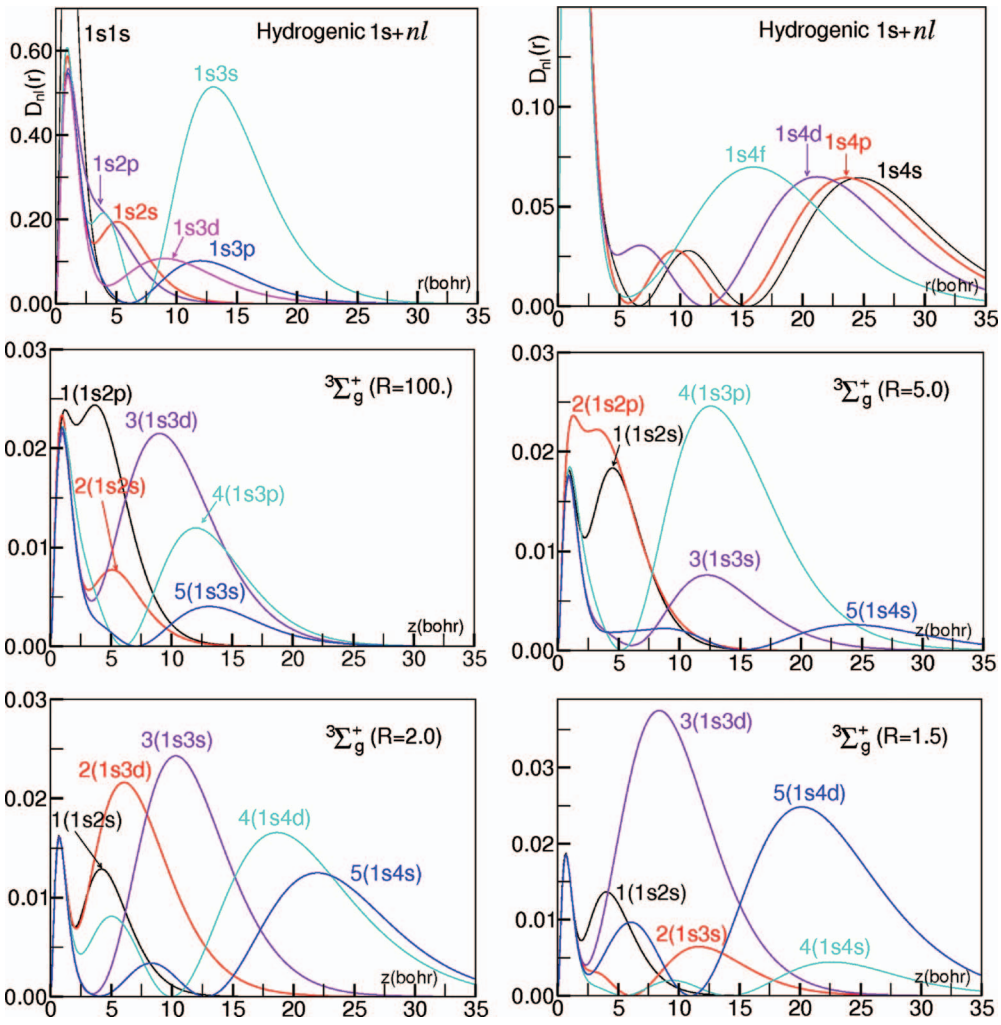

FIG. 8. Example of density distribution analysis for the first five $^3\Sigma_g^+$ states at internuclear distances of 100 5.0 2.0 and 1.5 bohrs.

Following the methodology developed in Refs. 1 and 2, in this section we analyze for the 14 $^3\Sigma_g^+$ states the dominant electronic configuration at different internuclear separations. This requires a recomputation of the state energies with subsets of the full basis set, starting, for example, with the *ns* subsets, then adding progressively the *np*, *nd*, *nf*, and *ng* subsets, thus finally reobtaining the state energies given in Fig. 3. The subsets in the order 1s, 2s, 2p, 3s, 3p, …, 5g are designated in this work as "canonically ordered subsets." This approach, named *subset decomposition*,[1,2] leads us to identify the prominent basis function for a given state energy at a given internuclear separation; thus it leads to a characterization of the electronic densities. Indeed, a given subset (or a combination of subsets) yields a number of states; by adding one or more subsets, the number of states increases, and those states previously obtained either retain the same energy or become more stable (our computational method is variational). In this way, one can detect the efficiency of a subset at a given internuclear separation for a given state.

A second technique used to analyze the electronic density is to consider for each state and for a few selected internuclear distances, the molecular radial distribution functions defined in Refs. 1 and 2 and denoted "state-$D_{nl}(r)$," namely, the molecular equivalent of the familiar probability distribution function $D_{nl}(r)$ in atoms.[23]

Recall that the radial distribution function for an atom with wave function $\Psi(r,\theta,\varphi)$ is $D_{nl}(r)=\Psi^2(r)r^2$.[23] We introduce a molecular function devised to represent the radial distribution function of an atom in a molecule, and for H_2 we consider the electronic density centered on one of the two H atoms, set at the origin of the coordinate system (the other atom being at $z=-R$). For a given *state* of H_2 and at a given internuclear distance *R*, we compute $\Psi^2(0,0,z)z^2$ for a set of z values, in the interval of zero to infinity. In analogy with the atomic computations of $D_{nl}(r)$, we consider the function $\Psi^2(0,0,z)z^2$ as a probability distribution function along the z axis for that H atom in H_2. The function is characteristic for a given state and for a given R value; for H_2 at a given R value, it is designated as $D_{state}(1s,nl)$ or simply state $(1s,nl)$. Clearly at $R=0$, the $D_{nl}(r)$ for a given helium state coincides with state $(1s,nl)$.

As reported in Ref. 1, the $D_{nl}(r)$s for H^- are notably different from those of the H or He atoms and resemble the 1s radial distribution but with a density nearly nodeless and with a slow decay toward zero density at large r values.

In Fig. 8, we give an example on the use of the $D_{state}(1s,nl)$ to analyze the electronic density at a given R value in a given state. In the top two insets, we report the density distributions obtained by adding hydrogenic $D_{1s}(r)$ to

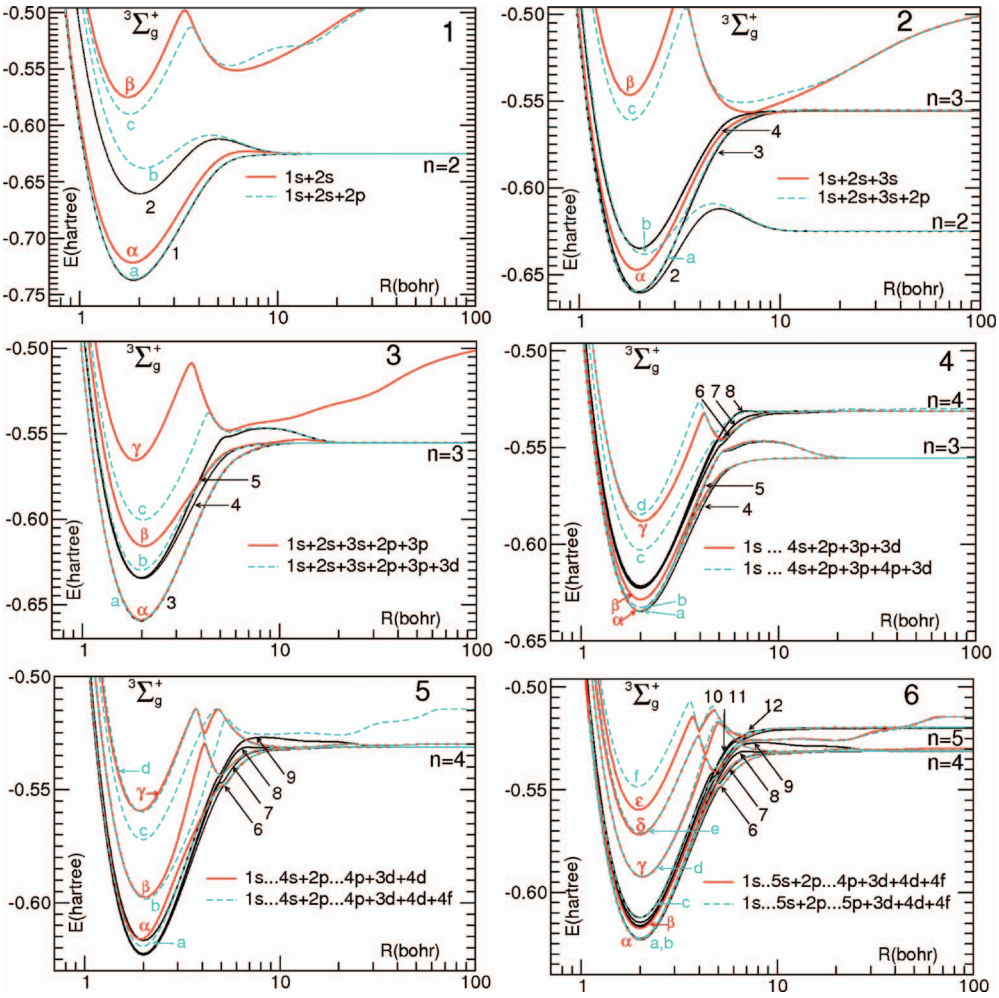

FIG. 9. Subset analysis for the $^3\Sigma_g^+$ states.

a $D_{nl}(r)$ with $nl=2s,\ldots,4f$. These composed distributions for the dissociation products $H(1s)+H(nl)$, identified by giving the nl value and by a specific color code, are our "reference distributions." In the insets of the second row, we report the computed state $(1s,nl)$ distributions at 100 and 5.0 bohrs, and in the third row those at 2.0 and 1.5 bohrs. The identification of a state $(1s,nl)$ distribution is obtained by comparing the number of nodes and the maximum positions (not the intensities) with the hydrogenic reference distributions. For each state we follow the characterization at each internuclear distance, for example, state 2 changes from 1s3s at 1.5 bohrs to 1s3d at 2.0 bohrs, to 1s2s at 5.0 bohrs, and finally to 1s2p at 100 bohrs. Note that $2(1s,nl)$ has 1s3s characterization at R=1.5 bohrs but 1s3d at R=2.0; whereas the $3(1s,nl)$ has 1s3d characterization at R=1.5 bohrs but 1s3s at R=2.0, an indication that a state crossing occurs. The $4(1s,nl)$ and $5(1s,nl)$ present an equivalent situation. This figure exemplifies changes in the state characterization and also eventual switches of characterization between two near states, an indication of strong state interactions and crossing. In general, from the distribution function analysis, we can recognize the characteristic atomic distributions from the united atom, $He(1s^1nl^1)$, to the dissociation products $H(1s^1)+H(nl^1)$ for covalent states or to the distributions $H^+H^-[^3S(1s^1nl^1)]$ present when the ionic component becomes relevant. Note that the identification becomes more and more problematic when the n value becomes higher due to the numerous nodes.

In the following, for each state, we report the subset decomposition analysis, followed by the radial distribution analysis, the latter performed at 14 internuclear separations, which sample the electronic density from the united atom to dissociation.

In Fig. 9 we analyze graphically the subset decompositions for the $^3\Sigma_g^+$ manifold. We present six insets, identified by numbers 1–6. In each inset, the energy curves are obtained from two different subset decompositions (differentiated with red and turquoise color curves) and compared to the few closely related final PECs (black curves; in the figure the superposition of two curves can result in degradation of the graphical representation). Starting with inset number 1 (dealing with the two subsets 1s+2s and 2s+2s+2p), the number of subsets is progressively increased nearly in canonical order.

A. State 1

The atomic states at the united atom and at dissociation are $He[^3S(1s2s)]$ and $H[^2S(1s^1)]+H[^2P(2p^1)]$, respectively. Inset 1 of Fig. 9 shows that the 1s+2s subset combination yields a number of states; we report the two lowest, desig-

nated as α and β. State α approximates the PEC of state 1; from short distances to about equilibrium it has a somewhat higher energy ($\sim$0.02 hartree) than the correct energy, but it dissociates correctly. State β is a very high energy double-well state. Addition of the 2p subset brings about a new set of states; we consider the three lowest, *a*, *b*, and *c*. State *a* realistically approximates state 1 (graphically superposed over the PEC of state 1). State *b* approximately reproduces state 2 (it is too high in energy; however it dissociates correctly); state *c* lowers the energy of state β and remains a double-well high energy state.

The radial distribution analysis yields a $1s^12s^1$ configuration from the united atom up to R=10 bohrs. From 15 bohrs to dissociation, the configuration is $1s^12p^1$. In the following we adopt the shorthand notation $1snl$ rather than $1s^1nl^1$.

B. State 2

The atomic states at the united atom and at dissociation are $He[^3S(1s3s)]$ and $H[^2S(1s^1)]+H[^2S(2s^1)]$, respectively. By considering the subsets 1s+2s+3s (see inset 2), we obtain the states α and β. State α is midway between states 3 and 4; β is higher in energy, with a double minimum and dissociates with high *n* value. Addition of the 2p subset generates states *a*, *b*, and *c*. State *a* lowers the energy of state α and reproduces the minimum of state 2. State *b* nearly follows the PEC of state 4 from short distances to about equilibrium, then continues below state 4, crosses state *a*, and nearly reproduces the barrier of state 2 until it dissociates correctly. Thus, the basis functions to realistically reproduce states 1 and 2 are identified as 1s, 2s, 2p, and 3s.

The radial distribution analysis for state 2 reveals at short distances a 1s3s configuration merging into the united atom. At 2.0 bohrs, the configuration is 1s3d; then it has ionic character from 6.0 to 10 bohrs. From 15 bohrs until dissociation, the configuration is 1s2s.

C. State 3

The atomic states at the united atom and at dissociation are $He[^3D(1s3d)]$ and $H[^2S(1s^1)]+H[^2D(3d^1)]$, respectively. Inset 3 considers states obtained with two subsets: 1s+2s+3s+2p+3p yielding states α, β, and γ, and addition of the 3d subset yields states *a*, *b*, and *c*. States α and *a* coincide with state 3. States β and *b* are higher than state 4 and dissociate as $n=3$. States γ and *c* are higher energy double-well states, with state *c* correctly dissociating as $n=3$ and reproducing the barrier of state 5. State 3, like states α and *a*, at the united atom and at dissociation has configurations with functions retaining the same *n* value and for this reason presents no bump.[7]

The radial distribution analysis yields for state 3 at short distances the configuration 1s3d. At equilibrium, the predominant electronic configuration is 1s3s, which persists until 6.0 bohrs, where it switches to 1s3d, then to 1s3p until 30 bohrs. At dissociation, the configuration is 1s3d. The radial distribution functions confirm the crossing between states 2 and 3 in the interval of 1.9–2.0 bohrs (see also Fig. 8). From the computed total energies, the crossing occurs near 1.94 bohrs, with minimum energy difference of 129.39 cm^{-1} (which should be compared with the value of 130.96 cm^{-1} at the same distance in Ref. 9); this crossing was first discussed in Ref. 16.

D. States 4 and 5

The atomic states at the united atom and at dissociation are $He[^3S(1s^14s^1)]$ and $He[^3D(1s^14d^1)]$, $H[^2S(1s^1)]+H[^2P(3p^1)]$ and $H[^2S(1s^1)]+H[^2S(3s^1)]$, respectively. Insets 3 and 4 describe the subsets needed to reproduce states 4 and 5. The subset 1s+2s+3s+2p+3p+3d (see inset 3) leads to correct dissociation for states 3–5. From inset 4, addition of the 4s subset generates the three states α, β, and γ. State α correctly reproduces state 4, and state β approximates state 5. The addition of the 4p subset yields states *a*, *b*, *c*, and *d*. State *a* fully reproduces state 4; state *b* lowers state β, reproducing state 5. States *c* and *d* dissociate as $n=4$. This is a confirmation that the $4l$ subsets are needed to represent at short distances states, which dissociate as $n=3$. The switch from $4l$ to $3l$ functions (in states dissociating as $n=3$) is responsible for the kinks in the PECs and for the seemingly irregular IEP given in Fig. 7 in the region of 4–10 bohrs.

In summary, from the radial distribution analysis, state 4 has the configuration 1s4s at short distances, 1s4d from equilibrium to 4.0 bohrs; then it becomes 1s3s. At 6.0 bohrs, the configuration is 1s3p, then 1s3s, and thereafter it returns to 1s3p until dissociation. State 5 from the united atom to near equilibrium has configuration 1s4d; at equilibrium the configuration becomes 1s4s until 5.0 bohrs, where it becomes 1s4p; at 6.0 bohrs it switches to 1s3d, then 1s3p, 1s3d, ionic, and finally 1s3s until dissociation. Furthermore, the radial distribution functions nicely confirm the crossing between states 4 and 5 before equilibrium. From our total energy computations, the crossing occurs near 1.90 bohrs, where the minimum energy difference between the two states is 63.40 cm^{-1}; in Ref. 10 the smallest BO energy difference for these two states is 58.72 cm^{-1} and occurs at 1.895 bohrs.

E. States 6–9

At the united atom, these states have configurations $He[^3S(1s^15s^1)]$, $He[^3D(1s^15d^1)]$, $He[^3S(1s^15g^1)]$, and $He[^3D(1s^16s^1)]$, respectively, and dissociate as $H[^2S(1s^1)]$ plus $H[^2F(4f^1)]$, $H[^2D(4d^1)]$, $H[^2P(4p^1)]$, and $H[^2S(4s^1)]$, respectively. States 6–8 are close in energy until about 4 bohrs. The subset 1s+...+4s+2p+...+4p+3d+4d leads to states α, β, and γ, all above state 8 (see inset 5); β and γ are high energy states. Addition of the 4f subset brings about states *a*, *b*, *c*, and *d*; state *a* is still above state 8, state *b* is near state β, and states *c* and *d* are high energy states. Three states dissociate correctly as $n=4$ (see inset 5). Basis functions with $n=5$ are needed to correctly represent the minimum of states 6–9, as shown in inset 6. From this inset, we see that the addition of the 5s subset generates states α, β, γ, δ, and ε, all lowered in energy by the addition of the 5p subset. With this subset, states *a*, *b*, *c*, *d*, *e*, and *f* are generated. States *a* and *b* reproduce states 6 and 7. State *c* approximates state 8, state *d* is higher in energy than state 9, and states *e* and *f* dissociate as $n=5$.

The radial distribution analysis for states 6–9 shows that from dissociation to about R=6 bohrs, the states are characterized by orbitals with $n=4$. State 6 at 30 bohrs has configuration 1s4f, which persists until 10 bohrs, where it changes to 1s4d, and at 6 bohrs to 1s4s. At 4 bohrs, it is 1s4p; at 3.0 bohrs, it is 1s5d and merges into the state He[^{3}S(1s^{1}5s^1)] at the united atom. State 7 at 30 bohrs has configuration 1s4d; then it switches to 1s4f and 1s4s and finally becomes 1s4f from 4.0 to 2.0 bohrs. At this distance, it becomes 1s5g and then goes into the He[^{3}D(1s^{1}5d^1)] state at the united atom. State 8 at 30 bohrs has configuration 1s4s, at 6 bohrs it becomes 1s4f, at 4 bohrs it becomes 1s5s, and at 2.4 bohrs it becomes 1s5g until the united atom. State 9 at 30 bohrs has configuration 1s4s, at 6 bohrs it is 1s5s, and then 1s6s from 4.0 bohrs to the united atom. States 6 and 7 cross near 1.8 bohrs, where the smallest computed energy difference is 55.20 cm^{-1}.

F. States 10–14

At the united atom, these states have configurations He[^{3}S(1s^{1}6g^1)], He[^{3}D(1s^{1}6d^1)], He[^{3}S(1s^{1}7s^1)], He[^{3}D(1s^{1}7g^1)], and He[^{3}S(1s^{1}7d^1)], respectively, and dissociate as H[^{2}S(1s^1)] plus H[^{2}G(5g^1)], H[^{2}F(5f^1)], H[^{2}D(5d^1)], H[^{2}P(5p^1)], and H[^{2}S(5s^1)], respectively. The basis subsets of inset 6 are clearly insufficient, and the full basis set (see Fig. 3) is needed. For these states the radial distribution analysis becomes rather uncertain due to the large number of maxima partially overlapping one another, as expected from the radial distribution functions given in Refs. 1 and 2 (both for the united atom and dissociation).

The high state PECs at the united atom need high nl value functions (nl=7d for state 14, whereas the n value at dissociation is 5). Thus, the requirement of higher n values for the functions at equilibrium compared to those at dissociation is due to the united atom configuration affecting the electronic density from very short internuclear distances to the equilibrium region. There are many ways to decompose the full basis set into subsets, and above we have reported a simple but systematic subdivision.

We could have considered a finer subset decomposition, for example, subdividing the ns into $n\sigma_g$ and $n\sigma_u$ or np into $n\pi_u$ and $n\pi_g$. For example, by considering the two families of states generated by the 1s…5s basis subsets, one with only σ_g orbitals and the second with only σ_u orbitals, we find that the first family generates the minimum at 2.0 bohrs but dissociates incorrectly, while the second allows correct dissociation.

Equivalently, if we compare the states generated by the 1s…5s+2p…5p basis subsets and the states obtained by the same subsets but without configurations with σ_u and π_g orbitals, we find that the interaction of the bonding with the antibonding orbitals is a main cause for the formation of bumps and leads to correct dissociation in the $^3\Sigma_g^+$ manifold. A gross feature emerging from this analysis is that a state dissociating as H(1s)+H(nl) requires at least $N=[n(n+1)/2-(n-l-1)]$ canonically ordered subsets. Further, addition of subsets with higher n and l values increases the computational accuracy at the minimum. For example, considering inset 2, even state 2, dissociating as H(1s)+H(2s), requires not only the two subsets 1s and 2s but also the 2p, 3s, and 3d subsets.

V. ANALYSIS OF THE $^3\Sigma_u^+$ manifold

For these states, we continue in the six insets of Fig. 10, the subset analysis followed by the radial distribution analysis, performed at 14 internuclear separations.

A. State 1

The atomic states at the united atom and at dissociation are He[^{3}P(1s2p)] and H[^{2}S(1s^1)]+H[^{2}S(1s^1)], respectively. From inset 1 of Fig. 10 we see that the subsets 1s+2s generate state α, which closely represents state 1 (only partially reported to save space). There are two higher states, β and γ; the first approximates state 2 and correctly dissociates as $n=2$; the second is above state 3 and dissociates with a high n value. Addition of the 2p subset leads to three states a, b, and c; state a essentially coincides with state 1 and a van der Waals minimum starts to appear at about 8 bohrs (not reported in the inset; see Table IV); state b reproduces state 2; and state c is a higher state, which however dissociates as $n=2$, reproducing state 3 (from 6 bohrs to dissociation). From the radial distribution analysis, state 1 has configuration 1s2p in the united atom, and at 0.5 bohr; the configuration becomes a mixture of 1s and 2p at 1.0 bohr, and then becomes 1s1s until dissociation.

B. States 2 and 3

The atomic states at the united atom are He[^{3}P(1s3p)] and He[^{3}P(1s4p)], and at dissociation, H[^{2}S(1s^1)]+H[^{2}P(2p^1)] and H[^{2}S(1s^1)]+H[^{2}S(2s^1)], respectively. Addition of the 3s subset (see inset 2) leads to three states α, β, and γ; state α reproduces state 2. State β closely follows state 3; state γ is a high double minimum state above state 4. From the subsets 1s+2s+3s+2p+3p, we consider states a, b, c, and d. State a, very close to state α, nicely reproduces state 2; state b, very close to β, reproduces state 3; states c and d are high energy double minimum states dissociating as $n=3$. From this inset, we see clearly the formation of the ridge (energy bump followed by a shallow and shortly extended minimum) in the region of 4–5 bohrs. Notice also the apparent continuation of state γ into state β interrupted by an avoided state crossing, a feature preannounced in inset 1.

From the radial distribution analysis, state 2 has configuration 1s3p at the united atom and at 0.5 bohr. The configuration becomes 1s3d from 1.0 to 3.0 bohrs and then becomes 1s2s till 100 bohrs, but at 10 000 bohrs, it dissociates as 1s2p. The 3d maximum of the configuration 1s3d is notably deformed, nearly resembling a 2s function. State 3 has configuration 1s4p from the united atom until 1.0 bohr; then it becomes 1s4d till 2.4 bohrs, then 1s3s till 4–5 bohrs, and then becomes ionic until about 8–9 bohrs, finally becoming 1s2p until 100 bohrs, but at 10 000 bohrs it dissociates as 1s2s.

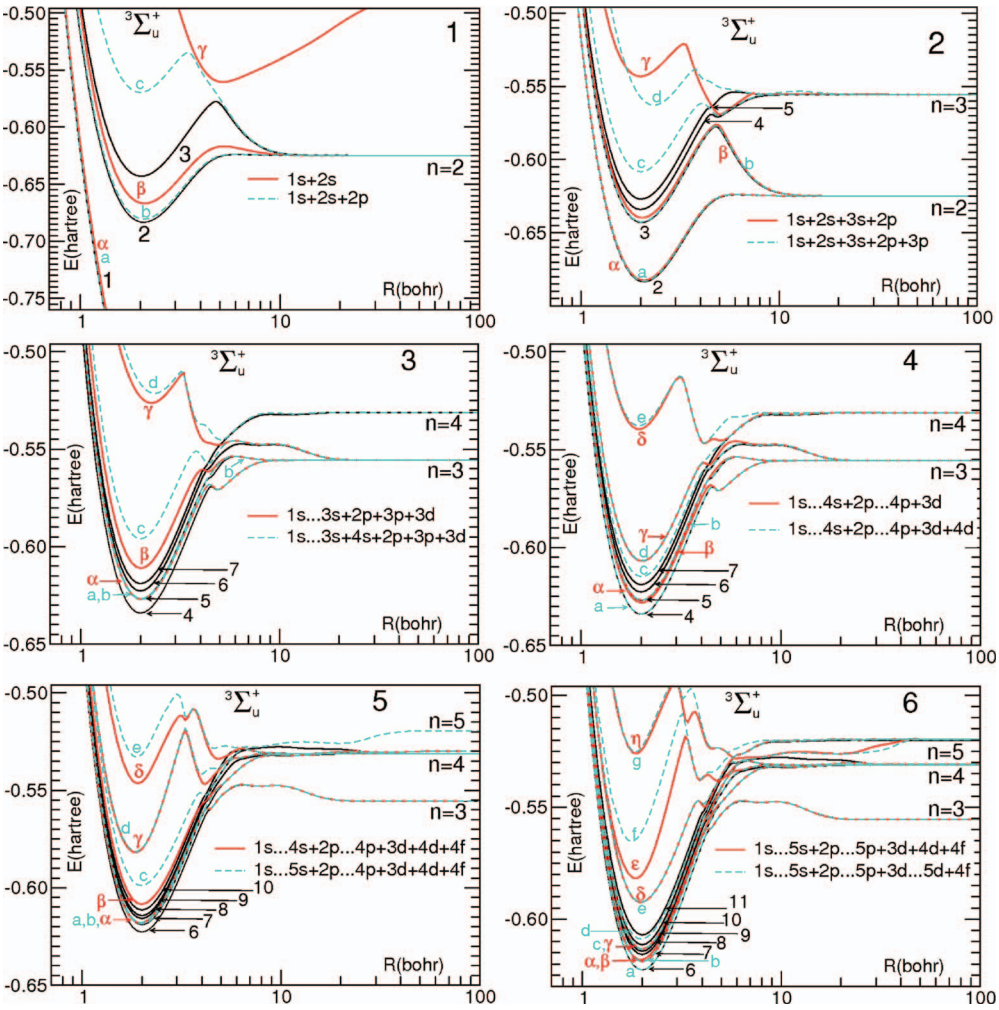

FIG. 10. Subset analysis for the $^3\Sigma_u^-$ states.

C. States 4–6

The atomic states at the united atom are He[^{3}F(1s4f)], He[^{3}P(1s5p)], and He[^{3}F(1s5f)], and at dissociation H[^{2}S($1s^1$)]+H[^{2}D($3d^1$)], H[^{2}S($1s^1$)]+H[^{2}P($3p^1$)], and H[^{2}S($1s^1$)]+H[^{2}S($3s^1$)], respectively. Inset 3 adds subset 3d to the subsets of inset 2, generating states α, β, and γ, and subset 4s generating the states a, b, c, and d. None of these reproduce the minima of state 4 or higher states, but the dissociations are correctly reproduced. Inset 4 adds first a 4p and then a 4d subset. With 4p, states α, β, γ, and δ are generated; with the 4d subset, states a, b, c, d, and e are generated. At this stage the ridge formation of the $^3\Sigma_u^+$ manifold is nearly correctly reproduced. State α nearly reproduces state 5; actually the 4d subset lowers it to state a, which reproduces state 4. State b reproduces state 5. All the remaining states in the insets are high in energy and correctly dissociate either to $n=3$ or $n=4$. Insets 3 and 4 provide a confirmation of the observation reported in the previous section, whereby the equilibrium region requires functions with principal quantum number n larger than those for dissociation.

From the radial distribution analysis, state 4 has configuration 1s4f from the united atom to about 2.4 bohrs; it switches to configurations 1s3p until 10 bohrs, where it becomes 1s3d until dissociation. State 5 has configuration 1s5p from the united atom until 4.0 bohrs; then it switches to 1s4f, 1s3s, and finally 1s3p. State 6 has configuration 1s5f from the united atom until 4.0 bohrs, then 1s3p at 5.0 bohrs, 1s3d at 6.0 bohrs, and is ionic from 8–9 to 15.0 bohrs. At 30.0 bohrs, the configuration is 1s3s until dissociation

D. States 7–10

The atomic states at the united atom are He[^{3}P(1s6p)], He[^{3}F(1s6f)], He[^{3}P(1s6h)], and He[^{3}F(1s7p)], at dissociation H[^{2}S($1s^1$)]+H[^{2}F($4f^1$)], H[^{2}S($1s^1$)]+H[^{2}D($4d^1$)], H[^{2}S($1s^1$)]+H[^{2}P($4p^1$)], and H[^{2}S($1s^1$)]+H[^{2}S($4s^1$)], respectively. From inset 5, the addition of the 4f and 5s subsets leads to states α, β, γ, and δ and a, b, c, d, and e, respectively. Only state 7 is reasonably reproduced by states α, a, and b; indeed states 6, 8, and 9 require functions higher than 5s. Inset 6 provides the 5p and 5d subsets, and consequently, states 6, 7, and 8 are reproduced by states a, b, and c, respectively. State d nearly reproduces state 9. From these insets we see, once more, that the dissociation is correctly obtained with functions of appropriate n values; these n values, however, are insufficiently high to correctly represent the region around the minima.

The radial distribution analysis for states 7–10 is nicely defined by the united atom configurations 1s6p, 1s6f, 1s6h

and 1s7p respectively, till 3.0 bohrs. In the region of 4–6 bohrs, the configurations are 1s5*l*, not easily distinguishable, since they are notably deformed relative to the reference configurations due to mixing of configurations. From 8.0 to 30 bohrs, the configurations are 1s4*l*; from 30 bohrs to dissociation, the configurations correspond to the atomic dissociation products.

E. States 11–15

The radial distribution analysis for states 11–15 is again represented by the united atom configurations He[^{3}P(1s7f)], He[^{3}F(1s7h)], He[^{3}P(1s8p)], He[^{3}F(1s8f)], and He[^{3}P(1s8h)], respectively, until 2.4 bohrs. The configurations of the dissociation products, [^{2}S(1s)]+H[^{2}G(5g)], H[^{2}S(1s)]+H[^{2}F(5f)], H[^{2}S(1s)]+H[^{2}D(5d)], H[^{2}S(1s)]+H[^{2}P(5p)], and H[^{2}S(1s)]+H[^{2}S(5s)], are predominant from about 30 bohrs to dissociation. In the region of 3.0–15.0 bohrs, the configurations 1sn*l* (with *n* from 5 to 9) are not easily recognizable since the radial distribution functions overlap with the many nodes and are deformed relative to the reference.

Note that from Fig. 10, a rather obvious computational pattern emerges for the $^3\Sigma_u^+$ manifold: as previously found for the $^3\Sigma_g^+$ states, to realistically reproduce a given state dissociating as H(1s)+H(*nl*), there is a need to include in the full CI computations canonically ordered subsets up to *nl* to correctly account for the dissociation products and subsets with larger *n* and *l* values to reproduce the equilibrium region.

As noted in the previous section, there are many different subset decompositions from those reported above, each bringing its own specific contribution to the understanding of the density variations occurring within each state. For example, we have considered the low states obtained either with the five *ns* subsets or with the nine *ns*+*np* subsets. The pattern emerging suggests that the manifolds in H_2 can be assumed to result from two systems of states. The first has minima at about 2 bohrs (same as for H_2^+) and follows a traditional pattern from short distances to about 4–5 bohrs, then tends to dissociate to states with values of *n* higher than the correct one. At about 4–5 bohrs, the first system interacts with the second system of states, leading to barriers and bumps leading to correct dissociation, represented by functions with *n* lower than the *n* value of the functions in the first system. Clearly, for the $^3\Sigma_u^+$ states one orbital always has *g* symmetry, and the other has *u* symmetry; thus the bonding and antibonding effects noted for the $^3\Sigma_g^+$ states are not relevant.

VI. CONCLUSIONS

We report the PECs for the H_2 states of the $^3\Sigma_g^+$ and $^3\Sigma_u^+$ manifolds, with electronic configuration $1s^1nl^1$ ($n=1-5$ and $l=0-4$), from R=0.01–10 000 bohrs. The determination of the 29 PECs is followed by a comprehensive and detailed energy and density analysis. Previous studies[9–13,20] were mainly limited to the first few excited states; this limitation leads to somewhat partial explanations for the irregularities in the manifolds occurring at about 4–6 bohrs.

The energies are obtained from full CI computations with extended and optimized STF and GTF basis sets using both Hartree–Fock and Heitler–London orbitals. The reliability of our PEC computations is verified by the good agreement with the best energies in the H_2 literature:[9–13] the energy deviations are between 10^{-5} and 10^{-6} hartree. Thus, our analysis is based on realistic wave functions and energy data. The total energies are quantitatively analyzed in terms of covalent and ionic contributions, and the percent of ionic energy is quantitatively determined for several states by comparing the total energy with its covalent component.

The electronic density evolution leading to incipient multiple minima is analyzed following the variations in the molecular distribution functions from the united atom to dissociation and via decomposition of the full basis set into subsets.

The complex pattern of the PECs at distances larger than 4 bohrs results from the multiple and complex transformations occurring in the electronic density due to state interactions and crossings. In particular, the pattern of PECs suggests that both the $^3\Sigma_g^+$ and $^3\Sigma_u^+$ manifolds in H_2 can be assumed to result from two interacting systems of states characterized by functions with different principal quantum numbers at dissociation distances less than that at equilibrium. The first system has minima at about 2 bohrs as for H_2^+ and follows a traditional pattern from the united atom, for short distances up to about 4 bohrs, then interacts with the second system of states leading to barriers and bumps followed by shallow minima. This second system of states, in order to dissociate correctly, requires functions with the *n* and *l* values of the separated atoms. The first system needs additional functions with higher *n* values to yield correct energy minima and to smoothly connect to the united atom, whose electronic configuration persists at internuclear distances even larger than equilibrium. In conclusion, systematic and comprehensive computations and analysis of the excited states with energy minimum below the H_2^+ ground state PEC are now available for the $^3\Sigma_g^+$ and $^3\Sigma_u^+$ manifolds in the H_2 molecule.

ACKNOWLEDGMENTS

It is a pleasure to acknowledge the use of the SMILES program by Jaime Fernandez Rico and his group. One of us (G.C.) acknowledges a grant from MIUR (Grant No. 2006030944).

[1] G. Corongiu and E. Clementi, J. Chem. Phys. **131**, 034301 (2009).
[2] G. Corongiu and E. Clementi, "Energy and density analyses of the $^1\Sigma_u^+$ states in the H_2 molecule: From the united atom to dissociation," J. Phys. Chem. (in press).
[3] G. Corongiu, J. Phys. Chem. **111**, 13611 (2007).
[4] J. Fernandez Rico, R. Lopez, I. Ema, and G. Ramirez, J. Comput. Chem. **25**, 1987 (2004).
[5] K. P. Huber and G. Herzberg, *Molecular Spectra and Molecular Structure IV. Constants of Diatomic Molecules* (Van Nostrand Reinhold, New York, 1979).
[6] G. Herzberg, *Molecular Spectra and Molecular Structure. 1. Spectra of Diatomic Molecules* (Van Nostrand, Toronto, 1950).
[7] R. S. Mulliken, J. Am. Chem. Soc. **88**, 1849 (1966).
[8] H. M. James and H. A. Coolidge, J. Chem. Phys. **1**, 825 (1933).
[9] G. Staszewska and L. Wolniewicz, J. Mol. Spectrosc. **212**, 208 (2002).
[10] W. Kolos and J. Rychlewski, J. Mol. Spectrosc. **177**, 146 (1996).

[11] T. Detmer, P. Schmelcher, and L. S. Cederbaum, J. Chem. Phys. **109**, 9694 (1998).
[12] J. W. Liu and S. Hagstrom, J. Phys. B **27**, L729 (1994).
[13] A. Preiskorn, G. C. Lie, D. Frye, and E. Clementi, J. Chem. Phys. **92**, 4941 (1990).
[14] A. Ishikawa, H. Nakashima, and H. Nakatsuji, J. Chem. Phys. **128**, 124103 (2008).
[15] F. Borondo, F. Martin, and M. Yanez, J. Chem. Phys. **86**, 4982 (1987).
[16] C. B. Wakefield and E. R. Davidson, J. Chem. Phys. **43**, 834 (1965).
[17] W. M. Wright and E. R. Davidson, J. Chem. Phys. **43**, 840 (1965).
[18] W. Kolos and L. Wolniewicz, J. Chem. Phys. **43**, 2429 (1965).
[19] W. Kolos and R. S. Mulliken, personal communication (1965) (see Ref. 7).
[20] S. Rothenberg and E. R. Davidson, J. Chem. Phys. **45**, 2560 (1966).
[21] P. O. Löwdin, Phys. Rev. **97**, 1474 (1955).
[22] G. Corongiu and E. Clementi (unpublished).
[23] L. Pauling, E. B. Wilson, *Introduction to Quantum Mechanics* (McGraw-Hill, New York, 1935).